Astronomy
&
Astrophysics

The VIMOS VLT Deep Survey

Public release of 1599 redshifts to $I_{AB} \leq 24$ across the Chandra Deep Field South[⋆]

O. Le Fèvre[1], G. Vettolani[2], S. Paltani[1], L. Tresse[1], G. Zamorani[5], V. Le Brun[1], C. Moreau[1],
D. Bottini[3], D. Maccagni[3], J. P. Picat[4], R. Scaramella[2], M. Scodeggio[3], A. Zanichelli[2], C. Adami[1], S. Arnouts[1],
S. Bardelli[5], M. Bolzonella[6], A. Cappi[5], S. Charlot[7,10], T. Contini[4], S. Foucaud[3], P. Franzetti[3], B. Garilli[3],
I. Gavignaud[4,11], L. Guzzo[8], O. Ilbert[1], A. Iovino[8], H. J. McCracken[7,12], D. Mancini[9], B. Marano[6], C. Marinoni[1],
G. Mathez[4], A. Mazure[1], B. Meneux[1], R. Merighi[5], R. Pellò[4], A. Pollo[8], L. Pozzetti[5], M. Radovich[9], E. Zucca[5],
M. Arnaboldi[9], M. Bondi[2], A. Bongiorno[6], G. Busarello[9], P. Ciliegi[5], L. Gregorini[2], Y. Mellier[7,12],
P. Merluzzi[9], V. Ripepi[9], and D. Rizzo[4]

[1] Laboratoire d'Astrophysique de Marseille – UMR 6110, OAMP, Université de Provence, Traverse du Siphon-Les trois Lucs,
   BP 8, 13376 Marseille Cedex 12, France
   e-mail: olivier.lefevre@oamp.fr
[2] IRA-INAF, via Gobetti 101, 40129 Bologna, Italy
[3] IASF-INAF, via Bassini 15, 20133 Milano, Italy
[4] Laboratoire d'Astrophysique de l'Observatoire Midi-Pyrénées – UMR 5572, 14 avenue E. Belin, 31400 Toulouse, France
[5] INAF – Osservatorio Astronomico di Bologna, via Ranzani 1, 40127 Bologna, Italy
[6] Università di Bologna, Dipartimento di Astronomia, via Ranzani 1, 40127 Bologna, Italy
[7] Institut d'Astrophysique de Paris – UMR 7095, 98bis bd Arago, 75014 Paris, France
[8] INAF – Osservatorio Astronomico di Brera, via Brera 28, 20121 Milano, Italy
[9] INAF – Osservatorio Astronomico di Capodimonte, Salita Moiariello 16, 80131 Napoli, Italy
[10] Max Planck Institut für Astrophysik, Karl-Schwarzschild-Strasse 1, 85741 Garching, Germany
[11] European Southern Observatory, Karl-Schwarzschild-Strasse 2, 85748 Garching, Germany
[12] Observatoire de Paris, LERMA – UMR 8112, 61 avenue de l'Observatoire, 75014 Paris, France

Abstract. This paper presents the VIMOS VLT Deep Survey around the Chandra Deep Field South (CDFS). We have measured
1599 new redshifts with VIMOS on the European Observatory Very Large Telescope – UT3, in an area 21×21.6 arcmin^2,
including 784 redshifts in the Hubble Space Telescope – Advanced Camera for Surveys GOODS area. 30% of all objects with
$I_{AB} = 24$ have been observed independently of magnitude, indicating that the sample is purely magnitude limited. We have
reached an unprecedented completeness level of 84% in terms of the ratio of secure measurements vs. observed objects, while
95% of all objects have a redshift measurement. A total of 1452 galaxies, 139 stars, 8 QSOs have a redshift identification, 141
of these being unsecure measurements. The redshift distribution down to $I_{AB} = 24$ is peaked at a median redshift $z = 0.73$, with
a significant high redshift tail extending up to ~4. Several high density peaks in the distribution of galaxies are identified. In
particular, the strong peak at $z = 0.735$ contains more than 130 galaxies in a velocity range ± 2000 km s^{-1} distributed all across
the transverse ~20 h^{-1} Mpc of the survey. We are releasing all redshifts to the community, along with the cross identification
with HST-ACS GOODS sources on the CENCOS database environment http://cencosw.oamp.fr.

Key words. surveys – galaxies: high-redshift – galaxies: distances and redshifts – cosmology: observations –
galaxies: evolution – cosmology: large scale structure of Universe

1. Introduction

Understanding the major steps in the evolution of galaxies still remains a major challenge to modern astrophysics. While

the general theoretical framework of the hierarchical growth of structures in the universe including the build up of galaxies is well in place (e.g. Peacock et al. 2004), at high redshifts this picture remains largely unconstrained by observations. The detailed properties of the main population of galaxies from large samples representative of the universe at various epochs

---

[⋆] The data presented in this paper has been obtained with the European Southern Observatory Very Large Telescope, Paranal, Chile.

remain to be established across most of the life of the universe beyond the large local volumes explored by the 2dFGRS (Colless et al. 2001) and the SDSS (Schneider et al. 2003), and expanding from smaller exploratory surveys (Lilly et al. 1995; Le Fèvre et al. 1995; Steidel et al. 2003; Cimatti et al. 2002).

The VIMOS VLT Deep Survey (VVDS) is a deep redshift survey aimed at studying the evolution of galaxies, large scale structures and AGNs over more than 90% of the current age of the universe. The unique feature of the VVDS is the simple magnitude selection applied to define a complete magnitude limited sample of distant galaxies, with a goal of more than 100 000 objects observed in multi-object spectroscopy. The VVDS rests on the observations of 5 different fields to smooth out the effects of cosmic variance when building the statistical properties of the galaxy population (Le Fèvre et al. 2004).

This paper presents the redshift survey observations of 1599 objects with $I_{AB} \leq 24$ conducted by the VVDS team around the Chandra Deep Field South (CDFS). The CDFS is field particularly rich of deep observations, starting from 1 Ms Chandra observations (Giacconi et al. 2002), including the HST-GOODS area (Giavalisco et al. 2004), as well as optical spectroscopy (Szokoly et al. 2003). The observations have been carried out with the VIsible Multi-Object Spectrograph (VIMOS) on the 8.2 m Melipal telescope of the European Southern Observatory Very Large Telescope. We are describing the processing steps and redshift measurements, and the associated quality control we have applied to these data. The content of the final catalog is detailed, as well as the cross identification with the Hubble Space Telescope Advanced Camera for Surveys GOODS images, and we present the main entries available from our interactive database. The main properties of the sample are briefly presented, including the redshift distribution of the sample.

2. Observations

2.1. Multi-Object Spectroscopy with VIMOS

Spectroscopic observations have been conducted with VIMOS on the VLT-UT3 Melipal (Le Fèvre et al. 2003). The low resolution red grism LRRED has been used with slits of 1 arcsec width. The spectral resolution in this mode is 34 Å at 7500 Å or $R \sim 220$. The spectral length has been limited by the red bandpass filter to 5500–9500 Å. Slits placed on objects have a typical length ~10 arcsec each.

2.2. VIMOS pointings

A complete VIMOS pointing is a combination of observations with the 4 quadrants of the instrument, each separated by a cross about 2 arcmin wide. With the above setup and the projected sky density of objects down to $I_{AB} = 24$, one VIMOS pointing allows to observe ~450 targets in one single observation (Le Fèvre et al. 2003).

We have set a total of 5 pointings around the Chandra Deep Field South, the positions are listed in Table 1. Together, they cover a total area of ~453$'^2$ including the complete
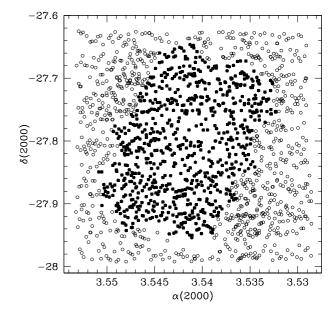

Fig. 1. Objects observed with VIMOS-VLT around the Chandra Deep Field South. Black circles are objects in the HST-ACS GOODS area.

HST-GOODS survey field (Giavalisco et al. 2004). The layout of observed galaxies is presented in Fig. 1.

2.3. Mask preparation

The preparation of slit masks for VIMOS observations has been done using the photometric catalog produced by the ESO Imaging Survey (EIS, Arnouts et al. 2001), and short images taken with VIMOS. The VIMOS images are used to produce a catalog of source positions in the VIMOS instrument coordinate system, which are then cross-correlated with the EIS catalog to compute the transformation matrix from the EIS catalog astrometric system to the VIMOS focal plane where slit masks are located. The VMMPS code was then run on the EIS catalog for all sources brighter than $I_{AB} = 24$ to optimize the number and positions of slits for each of the 4 masks per pointing. Masks have been cut by ESO Paranal Staff using the Mask Manufacturing Unit (Conti et al. 2001).

2.4. VIMOS observations

Observations with VIMOS have been obtained between October 31 and December 6, 2002. Observing conditions were photometric with an image quality between 0.6 and 1.2 arcsec FWHM. We have moved the telescope, hence the objects along the slits, in a sequence of 5 positions with offsets −1.4, −0.7, 0, +0.7, +1.4 arcsec from the reference pointing position. This is necessary to compute the fringing pattern produced above 8300 Å by the thinned EEV CCDs used in VIMOS, and remove it during processing.

Wavelength calibrations have been obtained during the day, observing Helium and Argon arc lamps through the observed masks. The spectrophotometric standard star LTT3218 has been used to derive the absolute flux calibration.

Table 1. Observed VIMOS pointings.

Pointing VVDS	α_{2000} (2000)	δ_{2000} (2000)	Date Observed	Number of slits	T_{exp} min
CDFS001	03h32m28.0s	$-27°48'30''$	31-Oct-02 1, 2, 4-Nov.-02	447	10×27
CDFS002	03h32m37.04s	$-27°50'30''$	5, 6-Nov.-02	331^a	8×27
CDFS003	03h32m18.95s	$-27°50'30''$	9, 10, 11, 12-Nov.-02	447	9×27
CDFS004	03h32m37.04s	$-27°46'30''$	27, 28, 29-Nov.-02 1, 2-Dec.-02	436	12×27
CDFS005	03h32m18.95s	$-27°46'30''$	2,4,5,6-Dec.-02	448	10×27

^{a} Quadrant 2 not observed.

3. Data Processing

Data processing has been conducted under the VIPGI environment developed by our team (Franzetti et al. 2004). VIPGI has been used to organize the multiple files and process all data from the raw 2D images and calibration to the production of sky subtracted, wavelength and flux calibrated 1D spectra. Because of instrument flexures not yet minimized at the time of these observations, the fringing pattern has been occasionally hard to remove. The quality control performed on these steps is described in Le Fèvre et al. (2004). The wavelength accuracy is better than ~1 Å rms all over the wavelength range, and the spectrophotometry is accurate to about 10%.

4. Redshift measurements

Measuring redshifts for a complete magnitude limited sample down to $I_{AB} = 24$ had never been attempted before our observations. The challenge is to measure redshifts over a large possible range $0 \leq z \leq \sim 5$, without any other a priori information than the magnitude selection. The approach we have followed involves an iterative build up of galaxy templates as observed with VIMOS, coupled to the powerful redshift measuring machine KBRED (Scaramella et al. 2004), based on cross correlation and principal component analysis methods. This approach has been applied and tuned on the more than 20 000 spectra obtained for the VVDS in the fall of 2002, and remained until recently very manpower intensive. On this critical step, we have enforced a very strict quality control.
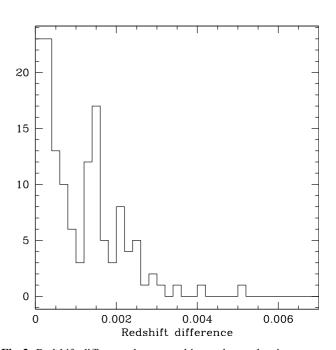
Each spectrum has been measured independently by 2 VVDS team members, and then compared. A final check has been done by a third team member prior to release into the database. Each spectrum is assigned a redshift, and a flag indicating the reliability level of the measurement, as defined in Le Fèvre et al. (1995) and described in Sect. 6. Flags 2, 3, 4 are the most secure, flag 1 is an indicative measurement based on continuum and few supporting features, and flag 0 indicates a measurement failure with no features identified. Flag 9 indicates that there is only one secure emission line tentatively assigned to the listed redshift (e.g. [OII]3727 Å or Hα).

Fig. 2. Redshift difference between objects observed twice or more in independent VIMOS observations. The distribution has a velocity dispersion $\sigma_z = 0.0012$ or 360 km s^{-1}, hence the accuracy in redshift measurement is $360/\sqrt{(2)} \sim 255$ km s^{-1}.

4.1. Redshift accuracy

The redshift accuracy can be estimated from a sample of 160 galaxies which have been observed twice with VIMOS within the 5 CDFS pointings. These galaxies have been included in two or more different mask sets, and observed independently at different times. The distribution of measured redshift differences is presented in Fig. 2. The dispersion of the redshift difference distribution is $\sigma = 0.0012$, or 360 km s^{-1}, hence the accuracy of a single redshift measurement is $360/\sqrt{(2)} \sim 255$ km s^{-1}.

We have compared our redshift measurements with the measurements of the K20 survey (Cimatti et al. 2002) and VLT-FORS2 measurements conducted by the ESO-GOODS team (www.eso.org/science/goods). A total of 70 objects have been observed both by the VVDS and the K20. For the 63 VVDS objects with flags ≥ 1, the redshifts agree for ~87% of the sample with a $\Delta z = -0.0004$ and $\sigma_z = 0.0017$, with the main disagreement concentrated on flag 1, as expected.
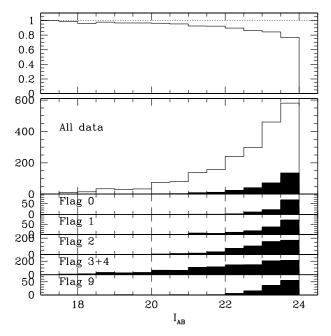
Fig. 3. Completeness of the $I_{AB} \leq 24$ sample. (*Top panel*) the fraction of secure redshift measurements and all measurements . The overall redshift measurement completeness is 84% with redshifts measurements for 95% of the sample. (*Middle panel*) The magnitude distribution of galaxies with secure redshift measurements (open histogram), and failed measurements (filled histogram). See text for the statistical computation of the failed measurements. (*Lower panels*) magnitude distribution of the galaxies for each of the quality flags.

The comparison with the ESO-GOODS data yields 46 objects in common, of which 42 have a VVDS flag ≥1. The VVDS vs. ESO-GOODS redshifts agree for 66% of the sample with $\Delta z = -0.0006$ and $\sigma_z = 0.0013$. There are 48 objects in common between our observation an the observations of X-ray sources by Szokoly et al. (2003), and our redshifts agree on 85% of this special class of objects (Hasinger, private communication). The detailed comparison of VVDS redshift measurements with the measurements from these other teams will be presented in Le Fèvre et al. (2004) .

4.2. Completeness

We have defined the completeness of the measurements as the ratio between the actual redshifts measurements and the observed spectra. We have removed from the list of observed spectra those which have a clearly identified instrumental or data processing problem affecting the measurement, like e.g. the slit is behind the guide probe of the VLT-UT3, or the data processing with VIPGI failed to properly detect the object because of strong residual features from the sky/fringing corrections. This will be described in details in Le Fèvre et al. (2004).

We are presenting in Fig. 3 the completeness in redshift measurement vs. I_{AB} magnitude for all objects (galaxies, stars, QSOs), and the magnitude distribution of objects with flags 0, 1, 2, 3, 4, 9. The completness is computed taking into account the fraction of objects with a good redshift measurement
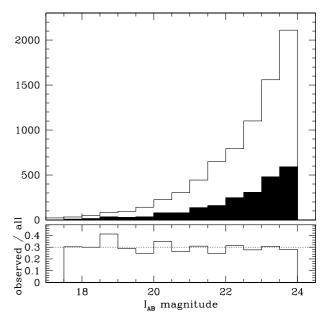

Fig. 4. (*Top panel*) I_{AB} magnitude distribution of objects observed with VIMOS in the Chandra Deep Field South (filled histogram), compared to the distribution of all objects in the area in the EIS photometric catalog (open histogram). (*Bottom panel*) The ratio of observed vs. all objects is 0.3.

for each of our quality flags listed in Sect. 7 (see Le Fèvre et al. 2004 for a detailed discussion on completeness).

The overall redshift measurement completeness reaches 84%. The objects with a redshift measurement listed in the catalogs, flags 1, 2, 3, 4, 9, 11, 12, 13, 14, 19, represent 95% of the sample, excluding objects with flags 0.

5. Cross identification with HST-ACS GOODS sources

The cross identification of the objects observed from the EIS catalog and the objects detected by HST-ACS has been performed running a cross correlation of our target list with the list of objects published in the version r1.0, December 22, 2003, of the GOODS survey multi-band catalog. The relative astrometry of the EIS vs. GOODS catalogs has been found to be extremely good, to within 0.1 arcsec over our survey field. A search circle with radius 0.3 arcsec has been used to search for HST sources corresponding to the ground based sources. This produced a matched list with only one to one identifications, and no double identifications.

6. Basic properties of the sample

6.1. Magnitude distribution

The magnitude distribution of objects observed in our survey is shown in Fig. 4 compared to the distribution of all objects in the EIS photometric catalog over the same area. We have observed 30% of all objects with $I_{AB} \leq 24$ in the area covered by the survey, independently of magnitude, as shown in Fig. 4. This demonstrates that there is no magnitude – dependent bias in our object selection and that our sample is purely magnitude
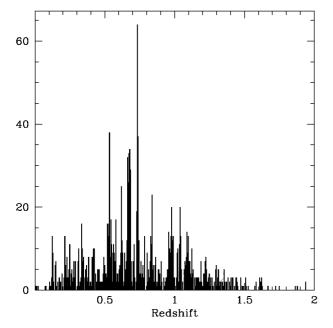
Fig. 5. Redshift distribution of galaxies with $I_{AB} \leq 24$ observed with VIMOS in the Chandra Deep Field South. The redshift bin is dz = 0.005. There are 42 objects identified with $z \geq 2$ not included in this figure.

selected even after the complex target selection in the making of the VIMOS multi-slit masks.

6.2. Redshift distribution

The redshift distribution (up to $z = 2$) of the full sample of galaxies and QSOs is presented in Fig. 5. The median of the redshift distribution is $\langle z \rangle = 0.73$. Galaxies are identified up to $z = 4.63$. As described in Le Fèvre et al. (2004) and Paltani et al. 2004, we have been successful in breaking into the "redshift desert" artificially produced by the difficulty to identify redshifts in the range $1.5 \leq z \leq 3$ due to our instrumental set-up, through extensive work on galaxy templates based on the high redshift galaxies measured in the VVDS (Paltani et al. 2004). We extensively discuss the incompleteness of the VVDS sample vs. redshift in Le Fèvre et al. (2004).

The strongest peaks in the distribution are at redshifts $z = 0.667$, and $z = 0.735$, confirming with better statistics the observations of Gilli et al. (2003). A total of 149 galaxies are measured in the $z = 0.667$ peak and 116 galaxies $z = 0.735$ peak. These structures are extending all across transverse ~16 Mpc of this survey ($z \sim 0.7$ ΛCDM with $H_0 = 70$, $\Omega_m = 0.3$, $\Omega_{Lambda} = 0.7$) in a wall-like pattern rather than in clusters. These peaks are also traced by X-ray sources as discussed by Szokoly et al. (2003).

6.3. Absolute magnitude and B–I distributions vs. redshift

The absolute magnitude M_B vs. redshift distribution is presented in Fig. 6. The absolute magnitudes have been computed based on $k(z)$ corrections derived from the fitting of the broad band photometry using rest frame galaxy templates
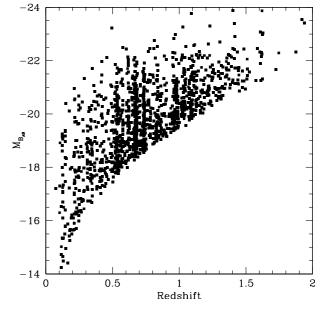

Fig. 6. Absolute $M_{B_{AB}}$ magnitude – redshift distribution for the full VVDS–CDFS sample
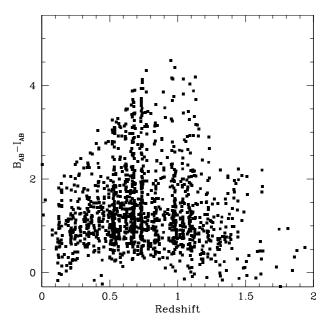

Fig. 7. $B_{AB} - I_{AB}$ vs. redshift distribution for the full VVDS–CDFS sample

(see Ilbert et al. 2004). The $B_{AB} - I_{AB}$ vs. redshift distribution is presented in Fig. 7

7. The CDFS catalog

Our catalog contains 1599 spectra including 1452 galaxies, 139 stars, and 8 QSOs. We have listed for each observed object:

– the ESO Imaging Survey identification number, equatorial coordinates α_{2000}, δ_{2000}, I_{AB} magnitudes and associated errors (Arnouts et al. 2001);
– the HST-GOODS identification number and $BVIz$ magnitudes and associated errors (Giavalisco et al. 2004);
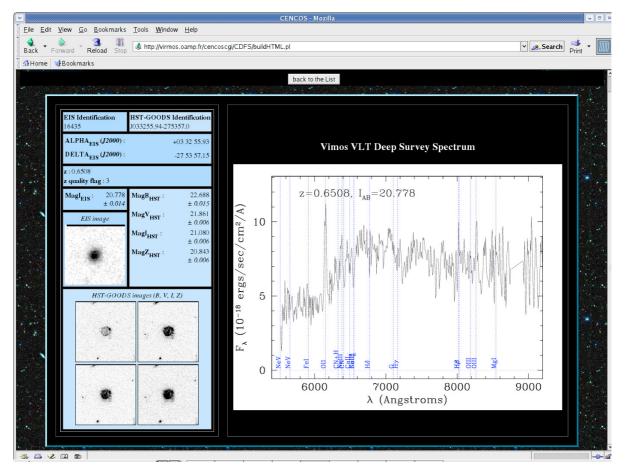
Fig. 8. Output from the VVDS-CDFS CENCOS database output panel for one single object. All information is presented, including the EIS and HST-GOODS identifiers, the ground based and HST-ACS magnitudes, the VVDS redshift and quality flag, and the HST-GOODS images and VVDS spectrum are displayed.

– the redshift measured by the VVDS team;
– the redshift quality flag (see Le Fèvre et al. 2004, for a detailed description). The flags definition taken from the Canada France Redshift Survey (Le Fèvre et al. 1995) is as follows:

0: no redshift could be measured;

1: some spectral features like e.g. weak line(s) or continuum break give a possible indication of the redshift (50–55%; of the redshifts are correct);

2: a few secure features are identified in support of the redshift measurement (80–85% of the redshifts are correct);

3: many secure features are identified (93–96% of the redshifts are correct);

4: strong secure features with high *S/N* are identified (98–99% of the redshifts are correct);

9: one secure emission line tentatively assigned to the listed redshift (e.g. [OII]3727 Å or Hα).

8. Public data release

We are publicly releasing all redshift measurements through the CENCOS (CENtre de COSmologie) database environment on our web site http://cencosw.oamp.fr with access to the database built under the Oracle environment. The catalog can be searched by coordinates, redshift interval, identification number in the EIS or GOODS catalogs, in combination with the spectra quality flags. Upon query, the database engine returns a list of targets, each of them can be examined in one single summary panel with all the VVDS spectroscopy information including the spectra, as well as the EIS and B, V, I, z HST-GOODS images, and associated photometry as shown in Fig. 8.

9. Summary

In the framework of the VIMOS VLT Deep Survey (VVDS), we have observed a large sample of galaxies around the Chandra Deep Field South, and are releasing the redshift data to the community. A total of 1599 objects with $I_{AB} \leq 24$ have a measured redshift. The completeness in redshift measurement for the targeted objects is high, above 84%. We find that the redshift distribution has a median of $z = 0.73$, with strong high density peaks observed across the field.

The combination of this redshift survey and the HST-ACS GOODS survey enables detailed studies of the evolution of galaxies in the Chandra Deep Field South.

the Szokoly et al. spectroscopy. The VLT-VIMOS observations have been carried out on garanteed time (GTO) allocated by the European Southern Observatory to the VIRMOS consortium, under a contractual agreement between the Centre National de la Recherche Scientifique of France, heading a consortium of French and Italian institutes, and ESO, to design, manufacture and test the VIMOS instrument.

References

Arnouts, S., Vandame, B., Benoist, C., et al. 2001, A&A, 379, 740

Cimatti, A., Daddi, E., Mignoli, M., et al. 2002, A&A, 381, L68

Colless, M. M., Dalton, G., Maddox, S., et al. 2001, MNRAS, 328, 1039

Conti, G., Mattaini, E., Maccagni, D., et al. 2001, PASP, 113, 452

Franzetti, P., Scoddegio, M., & the VVDS team 2004, A&A, in preparation

Giacconi, R., Zirm, A., Wang, J., et al. 2002, ApJS, 139, 369

Giavalisco, M., & GOODS team 2004, ApJ, 600, L93

Gilli, R., Cimati, A., Daddi, E., et al. 2003, ApJ, 592, 721

Ilbert, O., & the VVDS team, A&A, submitted

Le Fèvre, O., Crampton, D., Lilly, S. J., Hammer, F., & Tresse, L. 1995, ApJ, 455, 60

Le Fèvre, O., & the VVDS team 2003, The Messenger 111, 18

Le Fèvre, O., & the VVDS team 2004, A&A, submitted

Lilly, S. J., Le Fèvre, O., Crampton, D., Hammer, F., & Tresse, L. 1995, ApJ, 455, 50

Paltani, S., & the VVDS team 2004, in preparation

Peacock, J. 2002 Tenerife Winter School, Dark matter and dark energy in the universe [arXiv:astro-ph/0309240]

Scaramella, R., & the VVDS team 2004, in preparation

Steidel, C. C., Adelberger, K. L., Shapley, A. E., et al. 2003, ApJ, 592, 728

Schneider, D. P., Fan, X., Hall, P. B., et al. 2003, AJ, 126, 2579

Szokoly, G. P., Bergeron, J., Hasinger, G., et al. AJ, submitted, [arXiv:astro-ph/0312324]